LBL-37762
UC-410

Lawrence Berkeley Laboratory
UNIVERSITY OF CALIFORNIA

Accelerator & Fusion Research Division

To be presented at the National Conference on Synchrotron Radiation Instrumentation 1995, Argonne, IL, October 17–20, 1995, and to be published in the Proceedings

High-resolution Beamline 9.3.2 in the Energy Range 30–1500 eV at the Advanced Light Source: Design and Performance

Z. Hussain, W.R.A. Huff, S.A. Kellar, E.J. Moler, P.A. Heimann, W. McKinney, C. Cummings, T. Lauritzen, J.P. McKean, F.J. Palomares, H. Wu, Y. Zheng, H.A. Padmore, C.S. Fadley, and D.A. Shirley

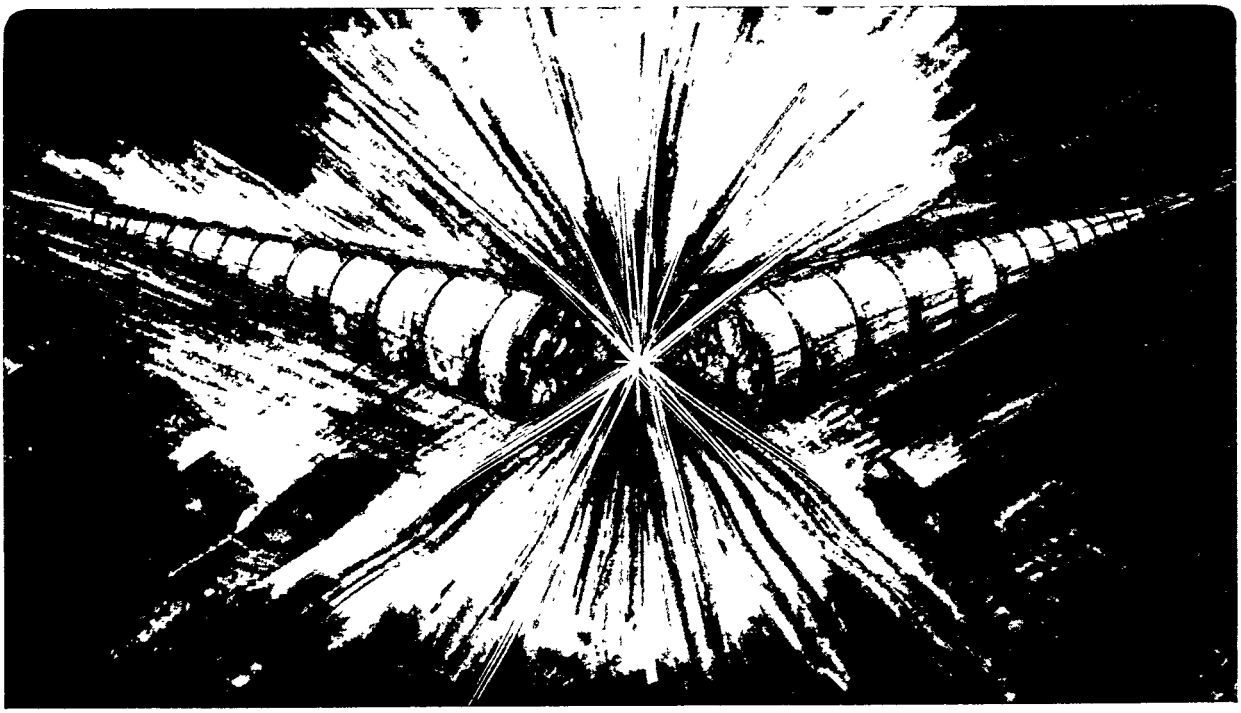

Prepared for the U.S. Department of Energy under Contract Number DE-AC03-76SF00098

High-Resolution Beamline 9.3.2 in the Energy Range 30-1500 eV at the Advanced Light Source: Design and Performance

Z. Hussain,[a] W.R.A. Huff,[a,b] S.A. Kellar,[a,b] E.J. Moler,[a,b] P.A. Heimann,[a] W. McKinney,[a] C. Cummings,[a] T. Lauritzen,[a] J.P. McKean,[a] F.J. Palomares,[a,c] H. Wu,[d] Y. Zheng,[d] H.A. Padmore,[a] C.S. Fadley,[a,c] D.A. Shirley[d]

[a]*Lawrence Berkeley National Laboratory, Berkeley, CA 94720*

[b]*The University of California, Dept. of Chemistry, Berkeley, CA 94720*

[c]*The University of California, Dept. of Physics, Davis, CA 95616*

[d]*The Pennsylvania State University, Dept. of Chemistry and Physics, University Park, PA 16802*

Keywords: Rowland Circle SGM
Circular Polarization
Active Feedback Beam Position Locking
Rotating Platform Endstation
Kirkpatrick-Baez Deflection Mirror Configuration

SRI '95 Abstract Number: D09

ABSTRACT

Bending magnet beamline 9.3.2 at the Advanced Light Source (ALS) was designed for high resolution spectroscopy with capability for delivering circularly polarized light in the soft X-ray energy region using three gratings. The monochromator is a fixed included angle spherical grating monochromator (SGM) and was originally used at SSRL as a prototype for later insertion device based monochromators for the ALS. For operation at the ALS, the toroidal pre-mirror used at SSRL was replaced by a horizontally focusing and a vertically focusing mirrors in the Kirkpatrick-Baez configuration.

Circularly polarized radiation is obtained by inserting a water-cooled movable aperture in front of the vertically focusing mirror to allow selecting the beam either above or below the horizontal plane. To maintain a stable beam intensity through the entrance slit, the photocurrent signals from the upper and lower jaws of the entrance slit are utilized to set a feedback loop with the vertically deflecting mirror piezoelectric drive. The beamline end station has a movable platform that accommodates two experimental chambers enabling the synchrotron radiation to be directed to either one of the two experimental chambers without breaking the vacuum.

1. INTRODUCTION

BL 9.3.2 is a 55 m Rowland circle SGM with movable entrance and exit slits installed on a bending magnet.[1,2,3] Fig. 1 is a schematic. Only those aspects which have not been described previously will be discussed in detail here. The vacuum chambers are supported by the ALS orthogonal six-strut system designed to withstand 1 g of lateral acceleration. The horizontally deflecting cylindrical pre-mirror focuses in the horizontal plane ~19 m from the mirror, which is ~3 m upstream from the center of the exit slit (S2) travel. The Kirkpatrick-Baez configuration[4,5] is completed by the vertically deflecting spherical mirror focusing in the vertical plane 8.4 m from the mirror which is at the center of the entrance slit (S1) travel.

Each slit is based on a flexure design allowing a side-driven micrometer to push the jaws open against spring tension continuously from ≤3 μm to 1500 μm maintaining the jaws parallel. S1 and S2 are translatable along the beam path by 600 mm and 1000 mm, respectively. This allows the Rowland circle condition to be satisfied over a wide energy range. A focus condition can be satisfied over the entire energy range of the monochromator.

Using one of three gratings, the accessible energy range is 30 eV to 1500 eV. The gratings are kinematically mounted onto a carriage attached to a rail by ball bearing rollers.[1] Each spherical grating is designed to have a 55 m radius. The fixed inclusion angle is 174°. The grating angle position is monitored by a laser interferometer.[1]

The refocusing mirror is a bendable cylinder with a fixed small radius (6.0 cm) and an adjustable large radius (80 m - ∞). The bending mechanism is based on a design by Howells[6] and will allow for moving the tangential focus from 1.5 m to ∞ from the refocusing mirror.

Satisfying the focus condition and closing S1 and S2 to 10 μm each, the resolving power is $E/\Delta E \geq 7{,}000$. Fig. 2 plots the $N_{2(g)}$ 1s to π^* resonance using first order light from the 600 l/mm grating. For this spectrum, the slit positions were set to satisfy the grating focus condition and remained fixed during the scan.

2. BEAMLINE ATTRIBUTES

Circular Polarization: Synchrotron radiation is linearly polarized with the polarization vector in the orbit plane. Viewing at any angle other than in the orbit plane, however, the perpendicular component of the polarization vector becomes non-zero. The net polarization is thus elliptical at any viewing angle other than in the orbit plane. The helicity of the elliptically polarized light changes when changing the viewing angle from above to below the orbit plane. Additionally, the degree of circular polarization increases as the out of plane viewing angle increases. Of course, the flux decreases for these larger angles. The optimum balance between circular polarization and flux within the limitations imposed by the beamline geometry must be determined before carrying out experiments using circularly polarized light.

Calculations were performed to determine how the degree of circular polarization and flux vary as a function of photon energy for different aperture positions introduced in the orbit plane to exclude the horizontal polarization component.[7] The parallel polarized component (s) is at a maximum in the orbit plane and the perpendicular polarized component (p) is zero in the orbit plane but maximum at a small angle (dependent on the photon energy) out of the plane. The beamline accepts radiation in the vertical direction from a lower angle, ψ_l, defined by the position of a movable aperture to an upper angle, ψ_u, defined by a mirror, a

grating, or a perhaps a real aperture. The flux through the aperture, F_a, is defined by

$$F_a = \int_{\psi_l}^{\psi_u} \frac{dF}{d\psi} d\psi \tag{1}$$

where $\frac{dF}{d\psi}$ is the flux per unit vertical aperture as a function of the out of plane angle ψ and depends on the machine energy, the photon energy, the critical photon energy, the bending field strength, as well as the s and p polarized light components.[8] Fig. 3 plots the calculated fraction of the total emitted flux accepted by the aperture. The half-apertures of the central stop are shown ranging from 0.0 to 0.5 mrads.

The degree of circular polarization, P_c, where

$$P_c = \sqrt{1 - \left(\frac{F_s - F_p}{F_s + F_p}\right)^2} \tag{2}$$

and F_s and F_p are the s and p polarized fluxes, respectively, was calculated as a weighted average of the circular polarization over the aperture. The weighting is due to the change in intensity of the s and p polarized components across the aperture. Thus,

$$\langle P_c \rangle_a = \frac{1}{F_a} \int_{\psi_l}^{\psi_u} P_c(\psi) \frac{dF}{d\psi} d\psi \tag{3}$$

Fig. 4 plots the calculated average degree of circular polarization for the aperture. For the largest stop size, the degree of circular polarization is greater than 0.9. Even with no stop, it is typically greater than 0.6 throughout the energy range.

To optimize the balance between the flux and the circular polarization, it is useful to calculate the merit function as described by

$$M = \langle P_c \rangle_a \sqrt{F_a / F_t} \tag{4}$$

where F_t is the total flux radiated by the source at the defined photon energy (see fig. 5). The half-apertures of the central stop are shown ranging from 0.0 to 0.5 mrads. The merit functions over the half-aperture sizes 0.0, 0.1, and 0.2 mrads are within 10% of each other over the entire energy range. This insensitivity is caused by the balance of decreasing flux and increasing degree of circular polarization.

A water-cooled aperture is installed upstream of the vertically deflecting mirror which can be positioned with 1 μm resolution to select the beam centroid for linearly polarized light. Alternatively, the aperture can be positioned above or below the beam center to select circularly or elliptically polarized light. A 0.5 mm slit below the selection aperture is used to determine the beam centroid; the radiation through this slit was measured to be 99% linearly polarized at the endstation.[9] The degree of circular polarization as measured at the endstation is over 0.8 at 700 eV with ≥30% of the total flux.[9]

Active Feedback on M2 Pitch: A beam position locking system was developed to correct for photon beam fluctuations. These may be caused by many factors, the most notable has been temperature variations of the low conductivity water (LCW) used to cool the ALS magnets and some optics. LCW temperature must not vary more than ±0.1 C° to maintain a stable photon beam.

The beamline is controlled by the Experimental Physics and Industrial Controls Systems (EPICS). The Proportional, Integral, and Derivative (PID) control algorithm in EPICS[10] is used for this beam position locking. The upper and

lower S1 jaws are electrically isolated from each other and from ground. The photocurrent from each jaw is monitored. This signal in conjunction with the PID logic is used to automatically adjust a piezoelectric drive which in turn changes the M2 pitch. The feedback routinely operates at 10 Hz.

Fig. 6 plots the error function, E_f, used for the feedback loop as a function of time. I_U and I_L indicate the photocurrent on the upper and lower jaws, respectively. Without the feedback loop in operation, the beam can drift causing the changes in the photocurrent collected from each jaw. However, when in operation, the feedback loop effectively locks the beam position thus stabilizing the flux at the endstation.

Rotating Platform Endstation: Mounted on a rotating platform are two different endstations. The platform rotates manually through 60° in <5 min. allowing the beam to be directed to either endstation without breaking the vacuum. The two halves of the platform are vibrationally decoupled from one another to allow assembly of one endstation while the other takes beam. The rotation stops have been designed to align the chambers upon successive rotations. For structural stability, the chambers are bolted to pods secured to the floor removing the 'drum-head' effect of the large platform.

Permanently mounted at station one is the Advanced Photoelectron Spectrometer/Diffractometer with an angle resolving Scienta SES 200 hemispherical electron energy analyzer for doing a variety of surface science experiments. These include high resolution photoelectron diffraction (scanned angle and/or energy) and x-ray photoelectron spectroscopy (XPS) of surfaces and interfaces. Additionally, magnetic circular dichroism (MCD) as well as x-ray total reflection XPS studies are being performed at station one.

Mounted at station two is the Applied Materials Chamber with a partial yield electron and fluorescence detector for NEXAFS and MCD studies. An angle integrating electron energy analyzer is used for XPS studies. Alternately mounted at station two is the Angle-Resolved PhotoEmission Spectrometer (ARPES) with a movable electrostatic hemispherical electron energy analyzer (mean radius of 50 mm) used for studying surfaces and interfaces. This system is mainly used for studying scanned energy photoelectron diffraction.

ACKNOWLEDGMENTS

The authors wish to thank H. Diamon, R. Ynzunza, Z. Wang, E. Tober, G. Andronaco, N. Hartman, and A. Adamson for help with the beamline construction. Additionally, the ALS support staff is crucial to the successful completion and operation of all beamlines. This work was supported by U.S. DOE contract number DE-AC03-76SF00098.

REFERENCES

[1]W.R. McKinney, M.R. Howells, T. Lauritzen, J. Chin, R. DiGennaro, E. Fong, W. Gath, J. Guigli. H. Hogrefe, J. Meneghetti, D. Plate, P.A. Heimann, L. Terminello, Z. Ji, D.A. Shirley, and F. Senf, Nuc. Instrum. and Meth. in Phys. Research, **A291** (1990)221-224.

[2]P.A. Heimann, F. Senf, W. McKinney, M. Howells, R.D. van Zee, L.J. Medhurst, T. Lauritzen, J. Chin, J. Meneghetti, W. Gath, H. Hogrefe, and D.A. Shirley, Physica Scripta **T31** (1990)127-130.

[3]Z. Hussain, W.R.A. Huff, S.A. Kellar, E.J. Moler, P.A. Heimann, W. McKinney, H.A. Padmore, C.S. Fadley, D.A. Shirley, J. of Elec. Spec. and Rel. Phenom. (in press).

[4]A.G. Michette, *Optical Systems for Soft X-Rays*, Plenum Press, New York, 1986.

[5]C. Kunz (ed.), *Topics in Current Physics: Synchrotron Radiation, Techniques and Applications*, Springer-Verlag, Berlin, Heidelberg (1979).

[6]M. Howells (unpublished).

[7]H.A. Padmore, Z. Hussain, and Y. Zheng, LSBL Publication #218.

[8]K. Green, in *Reference Documents for a National Synchrotron Light Source*, ed. J.P. Blewett, BNL 50595, Vol. 2, pp. 1-68, Brookhaven National Laboratory.

[9]J.B. Kortright, M.E. Rice Z. Hussain, H.A. Padmore, A. Adamson, W.R.A. Huff, E.J. Moler, S.A. Kellar, R.X. Ynzunza, F.J. Palomares, H. Daimon, E.D. Tober, and C.S. Fadley, Rev. Sci. Instrum. (in press) SRI 1995, USA.

[10]J.B. Anderson and M.R. Kraimer, *EPICS IOC Record Reference Manual*, Los Alamos National Laboratory, p. 103 (1992).

Hussain, et al., SRI '95 #D09

Figure 1: ALS Beamline 9.3.2 Schematic

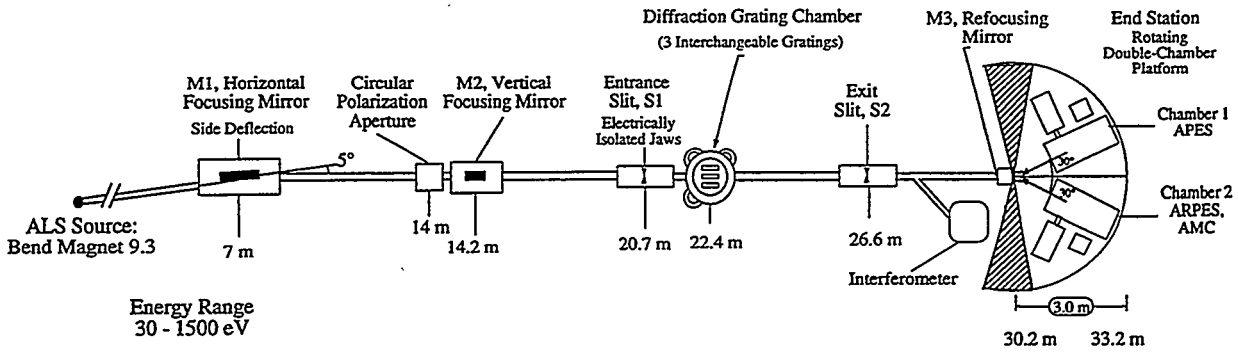

Hussain, et al., SRI '95 #D09

Figure 2: $N_{2(g)}$ 1s to π^*

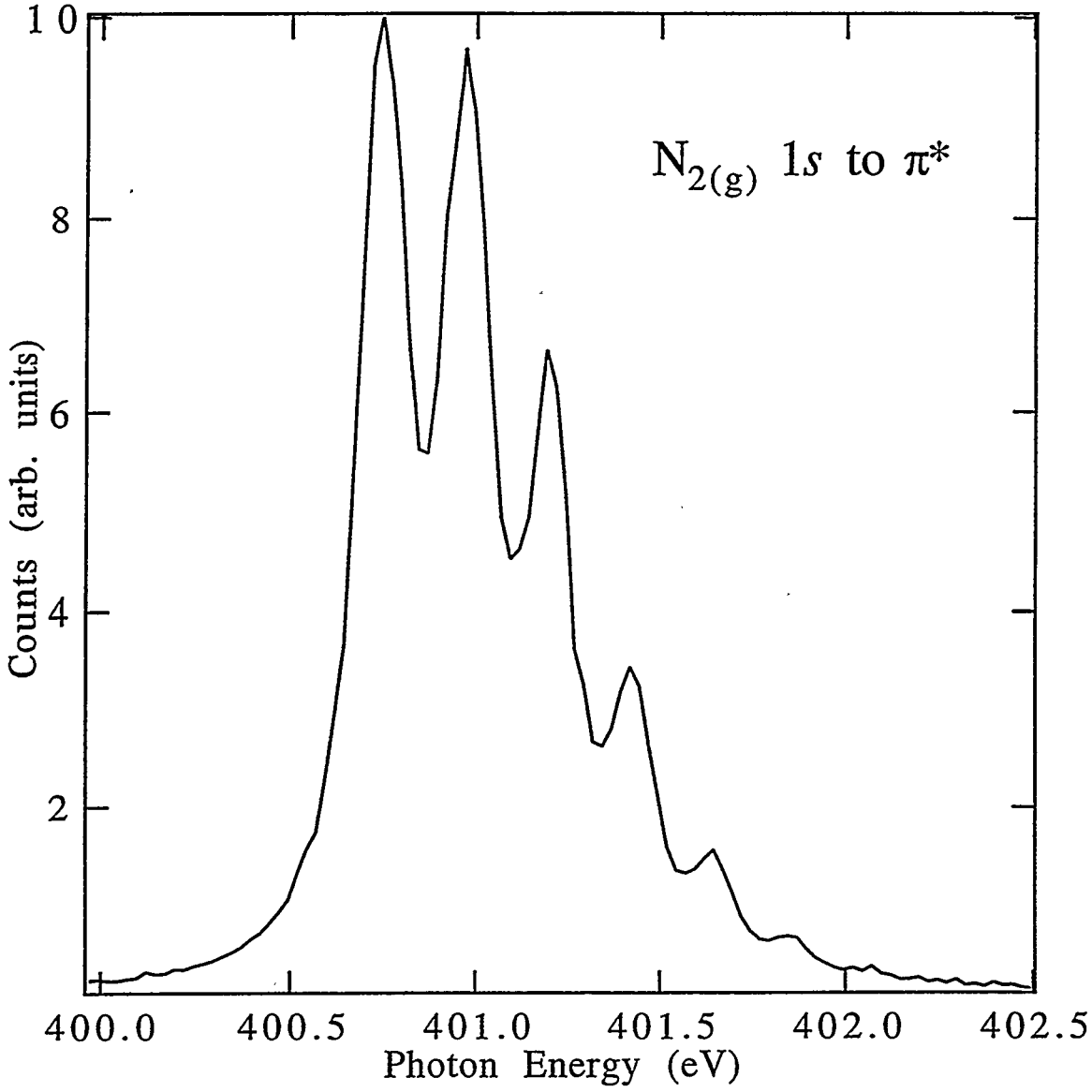

Hussain, et al., SRI '95 #D09

Figure 3: Calc. Fractional Flux vs. Photon Energy

Stop Half Apertures from 0.0 to 0.5 mrads

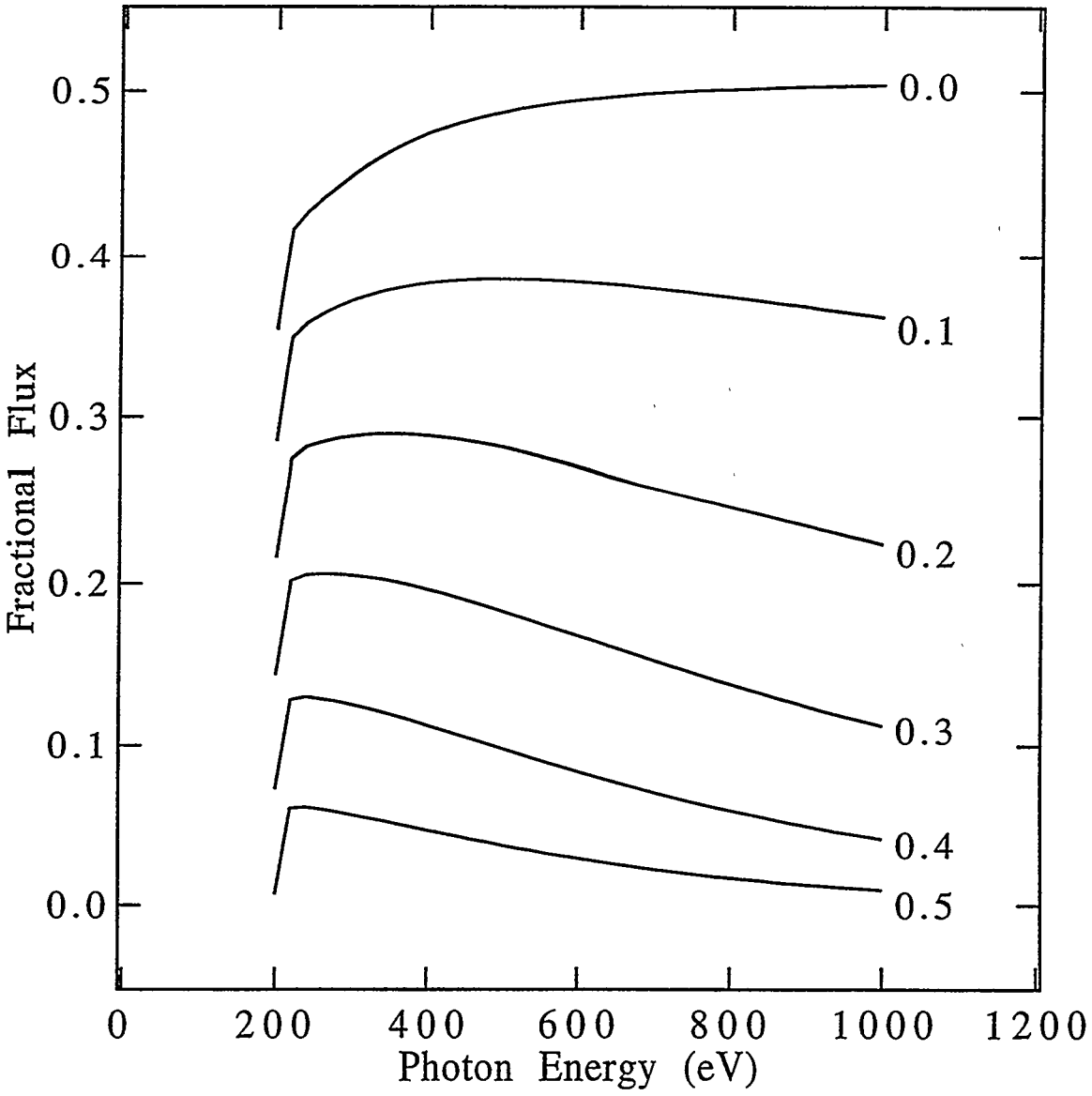

Hussain, et al., SRI '95 #D09

Figure 4: Calc. Avg. Degree of CP vs. Photon Energy

Stop Half Apertures from 0.0 to 0.5 mrads

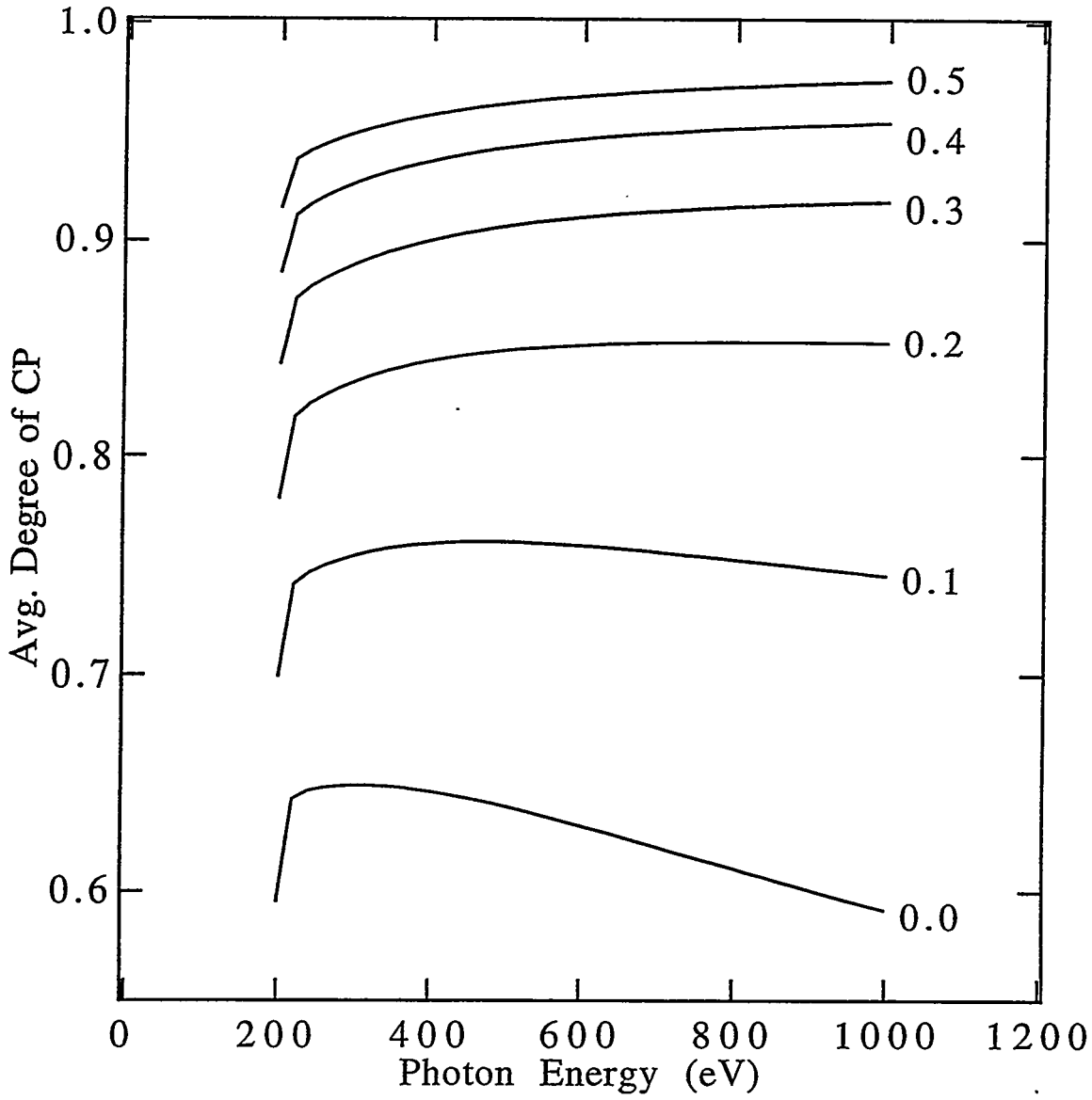

Hussain, et al., SRI '95 #D09

Figure 5: Calc. Merit Function vs. Photon Energy

Stop Half Apertures from 0.0 to 0.5 mrads

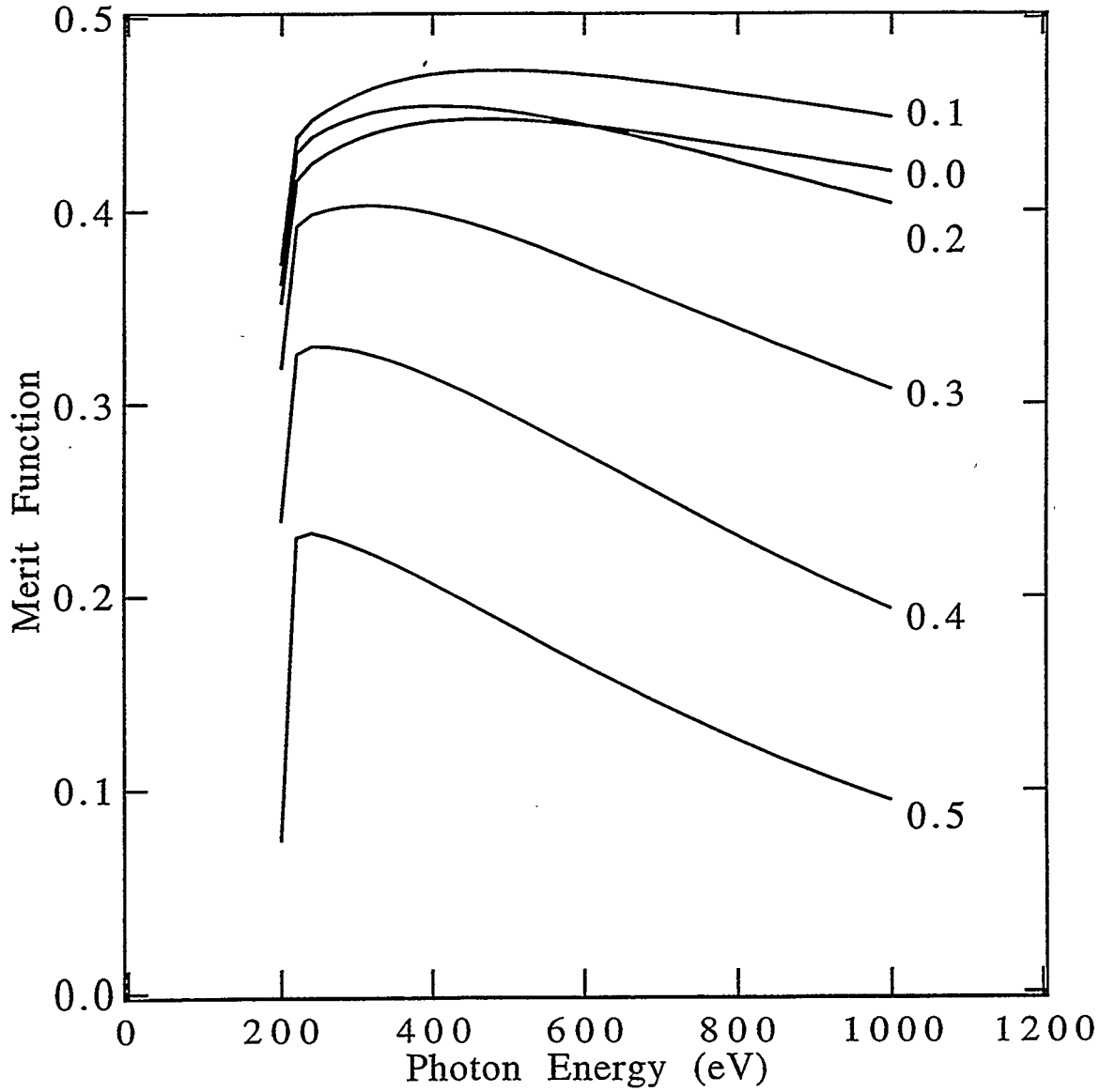

Hussain, et al., SRI '95 #D09

Figure 6: Plot of Error Function vs. Time

Illustrating Feedback Operation